Hardware and circuit design of a vibrational cleaner

Chin Fhong Soon[1,2], Kok Tung Thong[2], Kian Sek Tee[2], Nafarizal Nayan[1], Mohd Khairul Ahmad[1,2] Anis Nurashikin Nordin[3]

[1]Biosensor and Bioengineering Laboratory, MiNT-SRC, Universiti Tun Hussein Onn Malaysia, 86400 Parit Raja, Batu Pahat, Johor, Malaysia.
[2]Faculty of Electrical and Electronic Engineering, Universiti Tun Hussein Onn Malaysia, 86400 Parit Raja, Batu Pahat, Johor, Malaysia.
[3]Department of Electrical and Computer, Kulliyyah Engineering, International Islamic University Malaysia, 50728 Gombak, Selangor, Malaysia.

E-mail: soon@uthm.edu.my

Abstract. Microtissue can be grown on soft substrates of hydrogel or liquid crystal gel. These gels are adherent to the microtissues and they may interfere fluorescence imaging as background noise due to their absorbance property. A microfluidic vibrational cleaner with polydimethylsiloxane (PDMS) microfluidic chip platform was proposed and developed to remove the residual gel of liquid crystal adhered to the microtissues. The microtissues were placed in a microfluidic chip attaching to a microfluidic vibrational platform. In the system design, two motorised vibrators vibrating attached to a microfluidic platform and generating vibration signals at 148 Hz and 0.89 Grms to clean the microtissues. The acceleration of the vibration increased gradually from 0 to 0.96 Grms when the duty cycle of PWM pulses increased from 50 - 90%. It dropped slightly to 0.89 Grms at 100% duty cycle. Irrigation water valve was designed to control the fluid flow from water pump during cleaning process. Water pumps were included to flush the channels of the microfluidic device. The signals in controlling the pump, motor and valve were linearly proportional to the duty cycles of the pulse width modulation signals generated from a microcontroller.

1. Introduction

Culturing 3D cells on soft substrates such as hydrogel and liquid crystal gels are new emerging biotechniques in microtissue engineering [1-3]. 3D cell model is attracting scientific interest because of having potential applications in regenerative medicine, cancer therapy and drug development [4, 5]. In these scaffoldless techniques, cells are randomly distributed on the surface of the soft compliance substrates [6] and allowed to self-assemble into microspheroids or microtissues. To perform imaging of these microtissues, the microtissues must be removed from the liquid crystal (LC) surface of the soft substrates [2]. However, the removed microtissues are usually inevitably stained with adherent gel. For fluorescence imaging, these microtissues must be cleaned to avoid background interference to the optical signals [7].

Liquid crystal is a viscous material which is difficult to be removed. A previous study [8] demonstrated that solvent, temperature and vibration are effective to remove and clean the liquid crystal from glass substrate. The LC is not easy to be dissolved in common aqueous system and dissolution requires a solvent

such as isopropyl alcohol in water. The dissolution of a lipid gel is possible by the assistance of temperature. *Zhuang et al.* [8] indicated that LC exposed to high temperature contributed to better dissolving effect. However, the techniques proposed involved with harsh chemical or temperature that could be threatening to the viability of a living organism. Ultrasonic vibration is also a means for cleaning purpose [8]. Ultrasonic is formed by the shock waves of sound at frequencies above the human audibility [9]. 40 kHz of the ultrasonic wave is commonly applied in the manufacturing industry for surface cleaning [10]. Irradiation of ultrasonic in liquid can effectively removed the contaminants on the object surface by bubbles of cavitations [9]. Bubble of cavitations is the bubble implosions process caused by the generation of shockwave, impact and shear force. Bubbles with the presence of a lipid such as liquid crystals may damage the cell bilayer membrane. Among the methods discussed, cleaning based on mechanical vibration seemed to be a more viable technique to disperse the liquid crystal from the microtissues.

A microfluidic vibrational cleaner was demonstrated to be effective in the removal of the liquid crystal gel residue found on the keratinospheroids[11]. However, the hardware and circuit system design have not been reported. In this paper, we present a mechatronic system for generation of the vibrational cleaning with an aim to clean microtissues from the surface of the soft substrates.

2. Materials and method

2.1. Hardware development of the vibrational cleaner

This hardware system (Figure 1) comprises of four main parts that includes a control panel, microfluidic chip, water valve system and water pump system. The control panel was designed to be placed at the front panel of the system. The main intention was to keep a distance apart from the water reservoir. A liquid crystal display (LCD) was used to provide an interface to the operator. For the power supply, two units of 12Vdc sources were supplied to Arduino Mega 2560 R3 microcontroller and L298 motor driver module (Figure 3), respectively. The microcontroller was programmed to read the input commands from the buttons and variable resistors and adjust the pulse width modulated (PWM) output to drive the motorised vibrator accordingly. The duty cycle of the PWM is displayed on the LCD.

In the system, five variable resistors (VR) and four selection buttons were placed in an array next to the LCD. The PWM duty cycle of inlet water pump (IP), outlet water pump (OP), left motorised vibrator (V1) and right motorised vibrator (V2) were generated from the microcontroller and controlled by four variable resistors. The fifth variable resistor was used to vary the contrast of the LCD. Four selection functions are available on the control panel for selection of microtissues cleaning processes. The arrangement of function selections were initiated from Function 1, Function 2, emergency stop and reset buttons, respectively. Function 1 and 2 were assigned for cleaning microfluidic channel and samples in the microfluidic platform, respectively. A microfluidic platform was designed to hold the microtissues in a reservoir, and the input and output channels were used to supply and remove the fluid from the reservoir. Each of the two motorised vibrators (left and right) was attached to the terminal end of the microfluidic chip on the platform (Figure 2b). Figure 2a shows the simple design of a polydimethylsiloxane microfluidic chip with a circular reservoir for holding the microtissues.

The water pumps system consist of a pair of water pumps and beakers for distilled water and waste (Figure 1). Each water pump was placed on a customised water pump fixture customised with a tripod. Besides that, a beaker containing distilled water was placed at the bottom of water pump. The main inlet water pump was used to pump distilled water from the water storage beaker into the microfluidic device of the vibrational cleaning platform (Figure 2). The design of the microchip is as shown in Figure 2a. On the other hand, the waste water from the microfluidic vibrational cleaning system was extracted from the outlet of the microfluidic chip to the waste water beaker. For controlling the fluid flow to the microfluidic system, the vibrational cleaner has a modified drip irrigation water valve integrated to a microservo motor coupled with a shaft to control the amount of liquid dispensed into the microfluidic device.

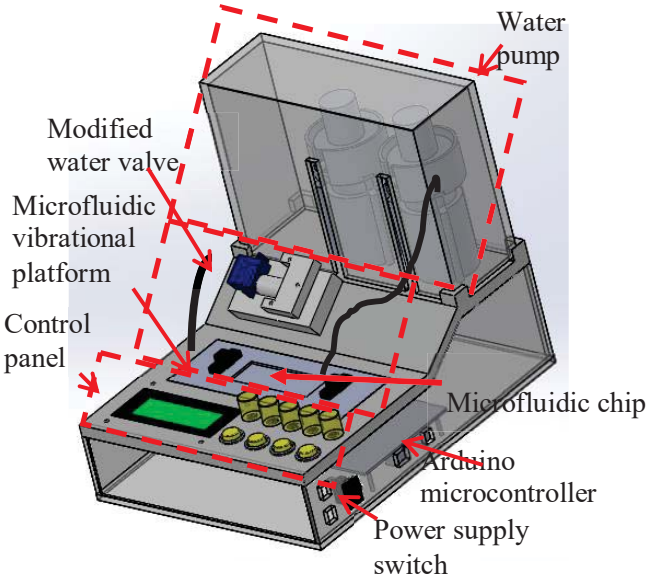

Figure 1. The conceptual design of customised microfluidic vibrational cleaner.

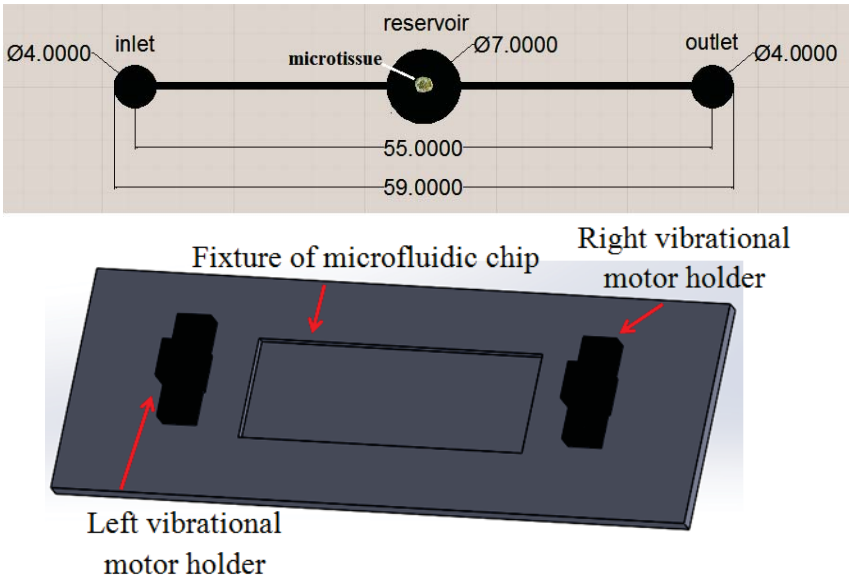

Figure 2. (a) Design of microfluidic chip. All units in mm. (B) The microfluidic vibration platform.

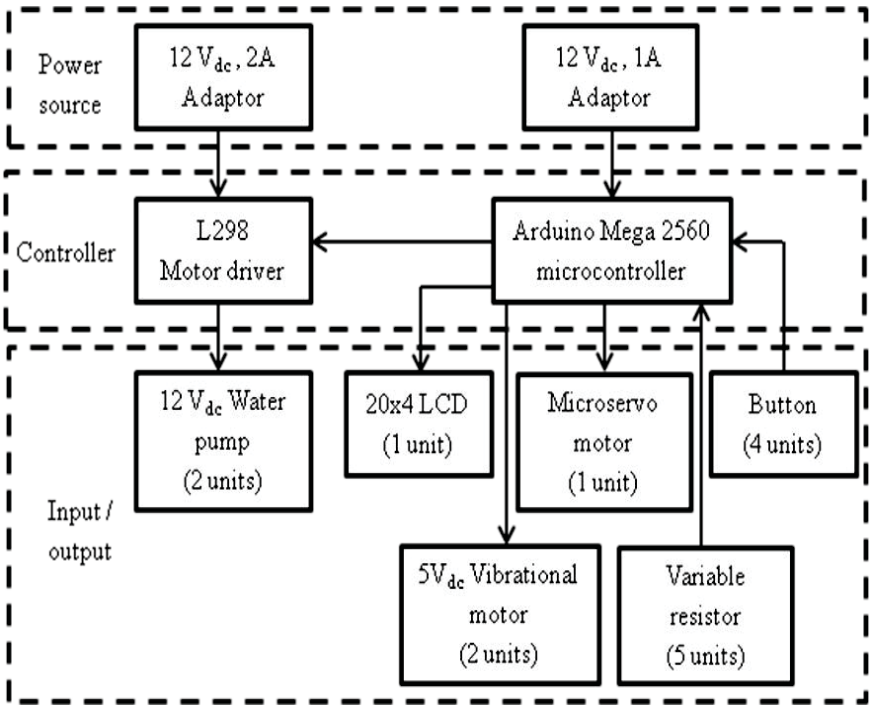

Figure 3. The block diagram of a microfluidic vibrational cleaner

2.2. Circuit design of the microfluidic based vibrational cleaner

The vibrational cleaning system comprises of an Arduino Mega 2560 R3 microcontroller, L298 motor drivers, 20 × 4 LCD, water pump, motorised vibrator, microservo motor for controlling irrigation water valve, variable resistor, push buttons and resistors as shown in Figure 4. All the circuit diagrams were designed using Proteus Design Suite 8.0. In the circuit diagram, push buttons and variable resistors are assigned to the input ports of the microcontroller. LCD, electrical water pump, electronic microservo motor and motorised vibrator are assigned to the output ports of the microcontroller. The water pump, motorised vibrator and microservo motor in the hardware were represented as dc motors (Figure 4). Each motor has a specific function in this project. Water pumps were used to extract or pump in the liquid for cleaning microtissues. Motorised vibrator was used to generate the vibration wave to clean the microtissues and the high output torque microservo motor controls the fluid dispensation to the reservoir.

The analogue inputs of the variable resistor from 0 to 5V were converted into 10-bits digital values from 0 to 1023 in the Arduino microcontroller and mapped to the duty cycle of the PWM signals varying from 0 to 100%. The analog input pins of the microcontroller (A1, A3, A5 and A7) were connected to the four variable resistors designated for regulating PWM signals out of the microcontroller to the two pairs of water pumps and vibration motors. Correspondingly, digital PWM pins (2, 3, 4, 5 and 6 of Figure 4) were connected to the inlet water pump, outlet water pump, left motorised vibrator, right motorised vibrator and water valve, respectively (Fig 4). Digital pins 21, 31, 32 and reset were connected to the four push buttons for program selections, whereas digital pins 48, 49, 50, 51, 52 and 53 were connected to the LCD configuration pins.

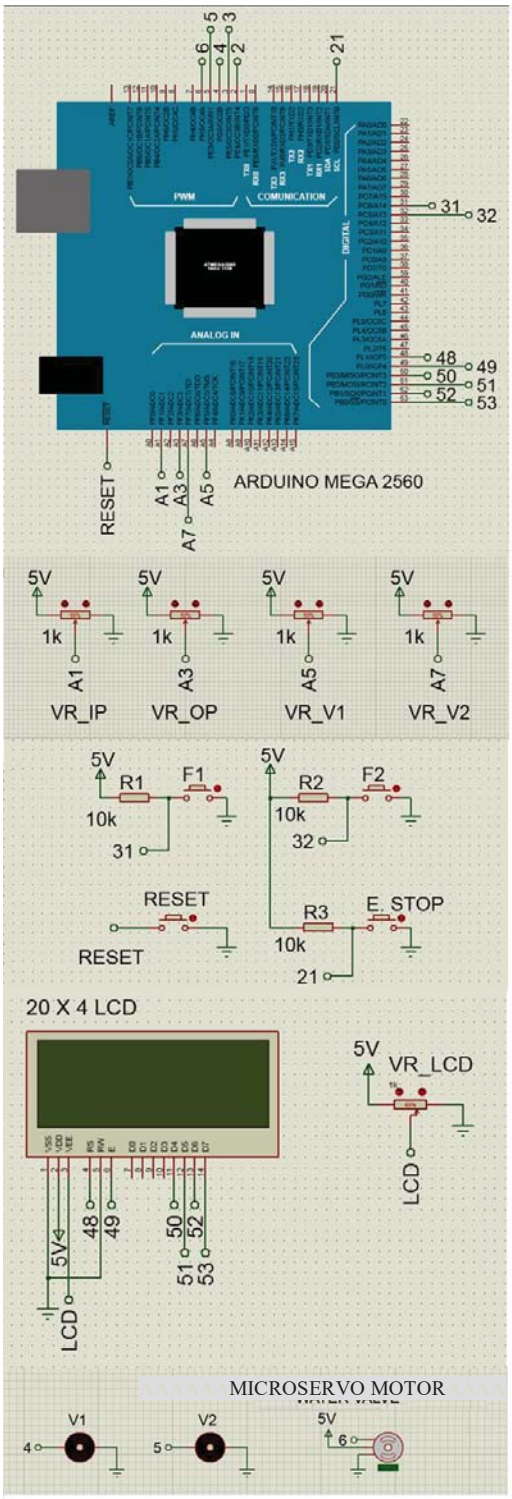

Figure 4. The schematic diagram of the microfluidic vibrational cleaner

A LCD was used to monitor and display the duty cycle percentage of the PWM pulses. Induction motor requires higher driving electric current, hence, a separate power supply was designed. A L298 motor driver module was used because of its operating supply voltage up to 46V, driving current up to 4A and it is included with an over temperature protection. Two external adaptors of 12 Vdc were used to supply power to the microcontroller and motor driver separately (Figure 5). Both grounds (GND) of the adaptor shared the same GND port to complete the close electric circuit. This module allows the control of two bi-directional motors. The rotation of motor was controlled by the configuration pins: IN1, IN2, IN3 and IN4 as shown in Figure 5. IN1 and IN2 pins were used to control the first motor rotation wheres, IN3 and IN4 for the second motor. The configuration for IN1 and IN2 of the motor driver module in controlling motor rotation is as shown in Table I. The enable pins were connected to the microcontroller's PWM ports (2 and 3) for controlling the motor rotation speed based on the PWM pulse. The OUT1, OUT2, OUT3 and OUT4 are outputs of the motor driver module connected to the motors of IP and OP (Figure 1).

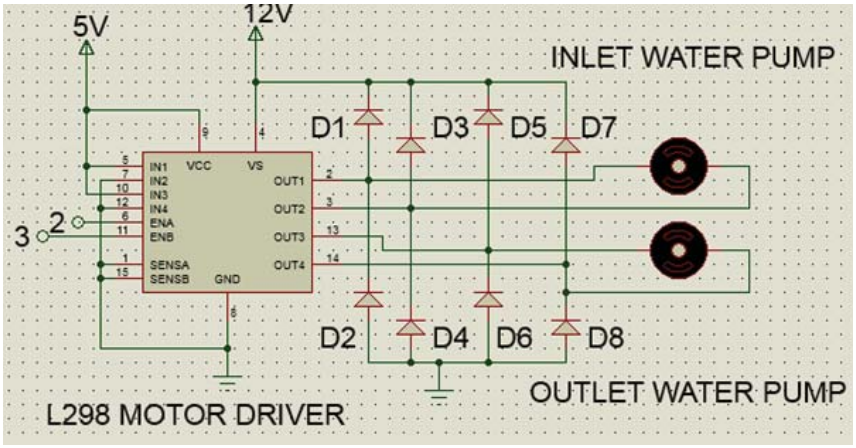

Figure 5. The circuit diagram for motor drivers and water pumps

A 180° TowerPro SG90 mini servo was selected as the irrigation water valve because the motor can precisely rotate the shaft in multiple degree of rotation up to 180° and performing higher power output. The application of this servo motor functions as an actuator in the system to control the modified water valve.

Motorised vibrator is an electric motor that generates vibration with an unbalanced mass on its drive shaft. It is a non-polarity motor which can rotate clockwise and anti-clockwise. The rotation direction of the motor is determined by the polarity of the voltage supply.

The vibration measurement of the microfluidic vibrational cleaner was conducted using a dynamic data logger (DEWETRON, DEWE-201) and was analysed in the DEWESoft 6.5.3 software. An accelerometer was attached to the microfluidic platform to detect the vibration frequency and acceleration. Dynamic data logger was used to record the vibration generated by the motor from 0 to 100% duty cycle of PWM pulses in one minute. The measurement of the vibration frequency and acceleration for each duty cycle percentage of the PWM output was repeated three times.

Table 1. Truth table for controlling motor rotation using a L296 motor driver module.

IN1	IN2	Motor rotation
0	0	Stop/brake
0	1	Clockwise
1	0	Anti-clockwise
1	1	Stop/brake

3. Results and discussion

3.1. The electronic output of the circuit

A 20 × 4 LCD was used to display the duty cycle of the PWM pulses (%) for each motor and the rotation angle (°) of the water valve (Figure 6). In the LCD, the name of the device was displayed on the first row. Second row displays the PWM percentage of inlet (IP) and outlet (IP) water pumps. The third row showed the left (V1) and right (V2) motorised vibrator's PWM percentage. The water valve rotation angle was displayed on the last row.

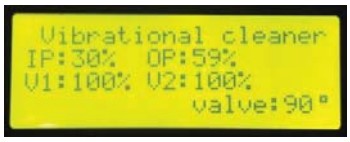

Figure 6. The LCD display

For determining the pulse width of the PWM, an Agilent digital storage oscilloscope (DSO-X 2022A) was used to obtain the waveform of the microcontroller. PWM is widely used on motor application due to the low power loss in the switching transistor and the flexibility in controlling motor speed. The PWM waveforms of 0, 20, 40, 60, 80 and 100% duty cycle for the water pump and motorised vibrator are as shown in Figure 7 and Figure 8, respectively. The waveforms showed that the amplitude and frequency for the inlet and outlet water pumps were similar at 12.5V and 2.439 kHz. The amplitude of both motorised vibrators was 5.1V at 2.439 kHz. The percentage and waveform output of the PWM increased proportionally with the variable resistor input.

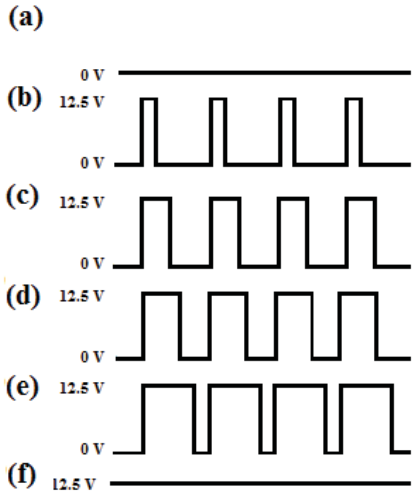

Figure 7. PWM waveform of water pump (a) 0%, (b) 20%, (c) 40%, (d) 60%, (e) 80% and (f) 100%

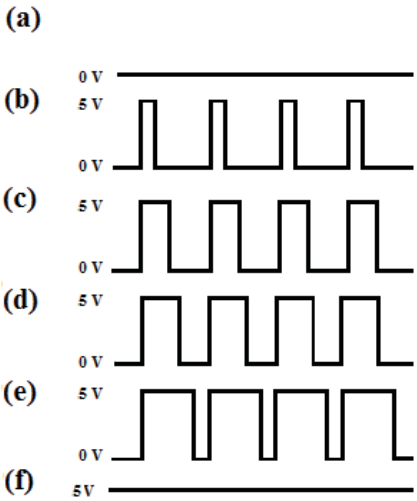

Figure 8. PWM waveforms of motorised vibrator (a) 0%, (b) 20%, (c) 40%, (d) 60%, (e) 80% and (f) 100%

3.2. The flow rate of the water pump

The inlet and outlet water pumps were found pumping at high flow rates (0 - 900 ml/min) as shown in Figure 9 and Figure 10. The flow rate of the water pump is linearly correlated with the duty cycle percentage of the PWM. The relationship of PWM pulse and the liquid flow rate of the microfluidic channel were similar for both water pumps. There was no liquid flow < 10% duty cycle of PWM due to the low flow rate which was insufficient to drive the water pump. At a minimum 10% duty cycle of PWM, the flow rate increased linearly with the percentage of PWM duty cycle. 40% of PWM duty cycle was selected for inlet water pump due to the implementation of back siphonage setup that needed low pressure to fill up the tube

at the water valve. In order to prevent back siphonage, the outlet water pump required higher duty cycle of PWM (60%) to extract the liquid from the reservoir.

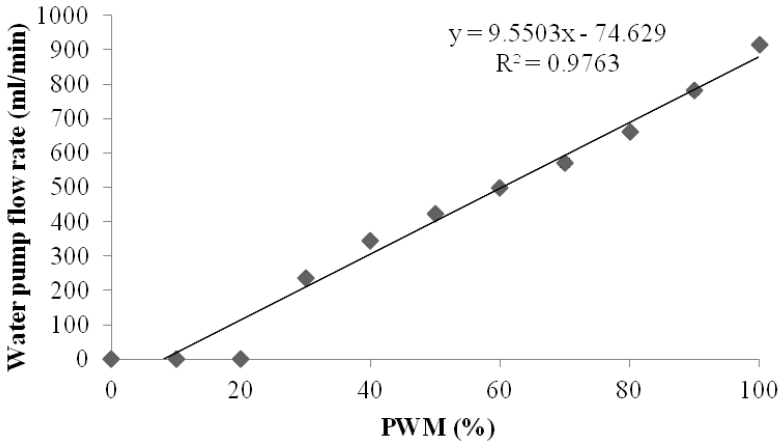

Figure 9. Liquid flow rate of inlet water pump.

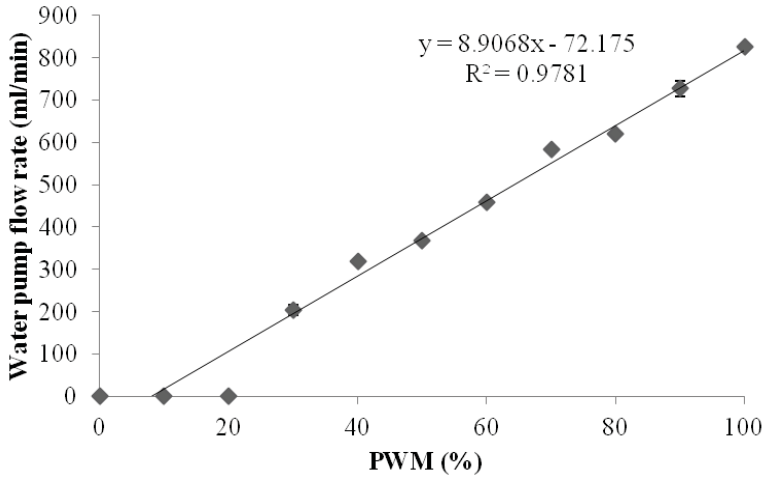

Figure 10. Liquid flow rate of outlet water pump.

3.3. The responses of the modified water valve

Water valve plays an important role to control the liquid flow into the microfluidic device with small and narrow channels. The system was designed to prevent the liquid from flowing into the microfluidic device during the cleaning process. Figure 11 shows the relationship between water valve rotation angle and liquid flow rate. The flow rate of the liquid decreased gradually from 28.28 ml/min (Θ = 0°) to 0 ml/min (Θ = 80°). The valve was fully shut at 80° to 140°. At rotation angle of 150° to 180°, the liquid flow rate increased again from 9 ml/min to 27.71 ml/min. The trend of the graph was not a perfect mirror due to the imperfect

mechanical design of the rotary shaft. However, the shaft was able to shut off the fluid from entering the microfluidic device effectively.

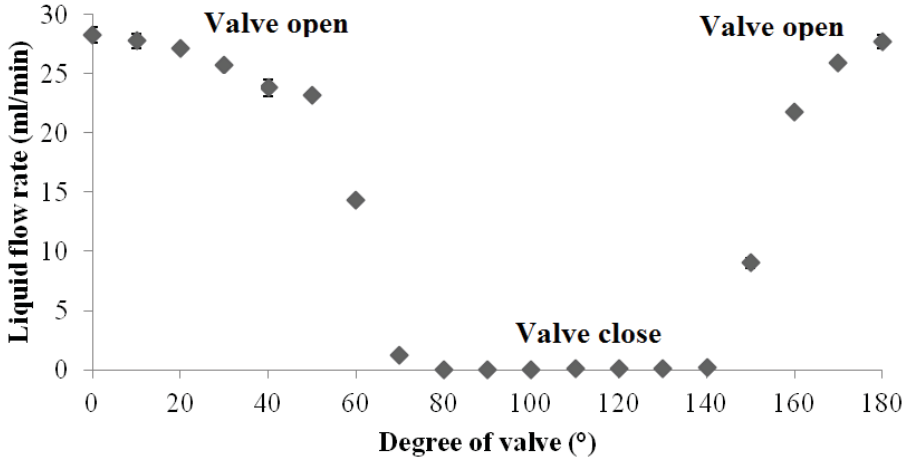

Figure 11. The liquid flow rate in responding to different rotation angle of the modified water valve.

3.4. The vibration frequency

The concept of the cleaning device was based on the random vibration generated by the motorised vibrator to remove the liquid crystal from microtissues. Figure 12 shows the relationship of the frequencies obtained from the microfluidic cleaning platform and duty cycle of the vibrational PWM pulse. Frequency obtained from the platform gradually increased when the motor PWM increased. The frequency range of the platform started from 59.57 Hz to 148.4 Hz. PWM of 10% and 20% duty cycle did not induce sufficient power to drive the motor. Hence, the vibration frequency remained at 60 Hz. The system requires PWM of at least 40 % duty cycle to generate higher vibration frequency.

Figure 13 shows the relationship of PWM pulse and the acceleration. Vibration acceleration tested for this system was below g-force, 1 Grms (low intensity). The acceleration increased gradually from 0 to 0.96 Grms when the duty cycle of PWM pulses increased from 50 - 90%. It dropped slightly to 0.89 Grms at 100% duty cycle. In this work, we found that the duty cycle of PWM which induced the vibration frequency is independent to the duty cycle of PWM correlated with the vibration intensity. Vibration frequency was a measurement of the revolution of motorised vibrator per second. Whereas, vibration intensity represented the energy dissipation of the vibration signal that was measured directly from the microfluidic platform via an accelerometer. For cleaning the gel off the microtissues, 148 Hz and 0.89 Grms were applied and recommended to clean microtissues to yield high survival rate of cells [11]. Previous studies showed that the vibrational frequency and acceleration applied did not affect the viability of cells and it may even improve the differentiation and metabolism of cells as suggested in [12, 13]. The current vibrational cleaning system in clearing the adherent LC gel from the microtissues was shown to be effective in oil film removal and the cells were viable as revealed by the live/dead cell stainings [10].

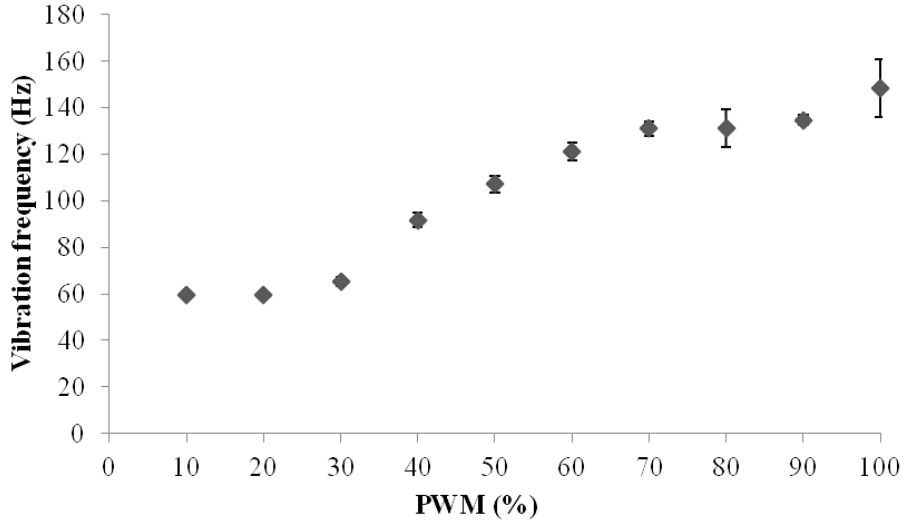

Figure 12. Vibration frequency versus motorised vibrator PWM (mean ± SD).

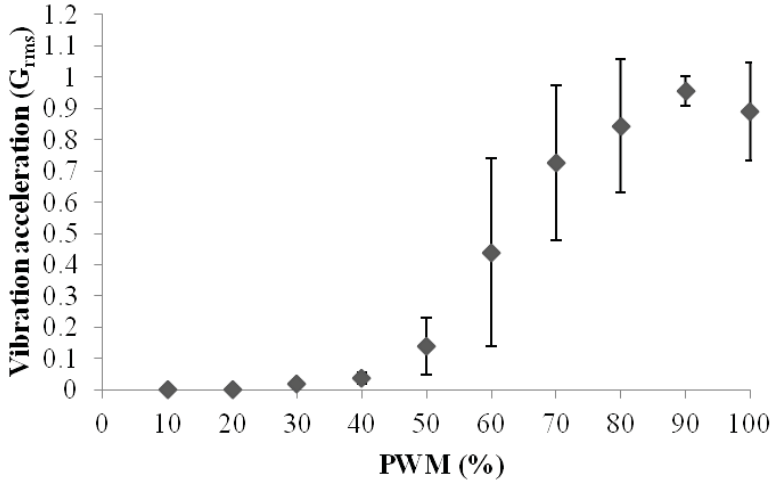

Figure 13. Vibration acceleration versus motorised vibrator PWM (mean ± SD).

4. Conclusion

A hardware and circuit system design for a vibrational cleaner has been described. This is a specialised system which is potentially applicable to clean any soft gels that adhered to microtissues in a microfluidic device. The vibrational system worked at different vibration frequencies and acceleration to provide mechanical vibration to disperse the gel in fluid. The system is also equipped with water pump system that automatic flushes water in and out of the microfluidic platform. The water valve effectively shut off the fluid from entering the microchannel during the vibration process. The water pumps and the motorised vibrators were working at similar frequency of 2.439 kHz but the speed were controlled by different duty cycles. The duty cycle of PWM which induced the vibration frequency is independent to the duty cycle of

PWM correlated with the vibration intensity because the latter was measured from the microfluidic platform.

Acknowledgement
The authors are grateful to the research financial support (Science Fund Vot No.: 0201-01-13-SF0104 or S024) awarded by Malaysia Ministry of Science and Technology (MOSTI).

References

[1] Vantangoli M, Madnick S, Huse S, Weston P and Boekelheide K 2015 MCF-7 human breast cancer cells form differentiated microtissues in scaffold-free hydrogels *PLoS ONE* **10** e0135426
[2] Soon C F, Thong K T, Tee K S, Ismail A B, Denyer M, Kong Y H, Vyomesh P and Cheong S C 2016 A scaffoldless technique for self-generation of 3D keratinospheroids on the liquid crystal surfaces *Biotech. Histochem.* **91** 283-95
[3] Kassim Y L, Tawil E A, Lecerf D, Couteau J, Simon T, Buquet C, Vannier J P and Demange E 2014 Biomimetic three dimensional cell Culturing: colorectal cancer micro-tissue engineering *Int. J. Clin. Oncol.* **3**
[4] Orive G, Hernández R M, Rodríguez A, Calafiore R, Chang T M S, de Vos P, Hortelano G, Hunkeler D, Lacík I and Pedraz J L 2003 History, challenges and perspectives of cell microencapsulation. *Trends Biotechnol.* **22** 87-92
[5] Hirschhaeusera F, Menneb H, Dittfeldc C, Westb J, Mueller-Kliesera W and Kunz-Schughartc L A 2010 Multicellular tumor spheroids: An underestimated tool is catching up again *J. Biotechnol.* **148** 3-15
[6] Soon C F, Ali Khaghani S, Youseffi M, Nayan N, Saim H, Britland S, Blagden N and Denyer M C T 2013 Interfacial study of cell adhesion to liquid crystals using widefield surface plasmon resonance microscopy *Col. and Sur. B: Bio.* **110** 156- 62
[7] Davis N E 2008 Highly modular protein polymers for multivalent display, liquid crystalline bacillary polymers and hydrogels for in situ tissue engineering. In: *Chemical and Biological Engineering*, (Ann Arbor: Northwestern University) p 235
[8] Zhuang X, He W, Li G, Huang J and Ye Y 2012 Materials separation from waste liquid crystal displays using combined physical methods *Polish Journal of Environmental Studies* **21** 1921-7
[9] Ensminger D 1988 *Ultrasonics: Fundamentals, Technology, Applications, Revised and Expanded*: CRC Press)
[10] Mason T, Cobley A, Graves J and Morgan D 2011 New evidence for the inverse dependence of mechanical and chemical effects on the frequency of ultrasound *Ultrasonics sonochemistry* **18** 226-30
[11] Thong K T, Soon C F, Ismail A B and Tee K S 2015 Development of a microfluidic vibrational cleaning system for cleaning microtissues *IFBME proceedings* **56** 155-8
[12] Tirkkonen L, Halonen H, Hyttinen J, Kuokkanen H, Sievänen H, Koivisto A-M, Mannerström B, Sándor G K, Suuronen R, Miettinen S and Haimi S 2011 The effects of vibration loading on adipose stem cell number, viability and differentiation towards bone-forming cells *Journal of The Royal Society Interface* **8** 1736-47
[13] Gaston J B, Quinchia R and al. e 2012 The response of vocal fold fibroblasts and mesenchymal stromal cells to vibration *PLoS One* **7** e30965-9